

Growth habits and defects in ZnO nanowires grown on GaN/sapphire substrates

Igor Levin, Albert Davydov, Babak Nikoobakht, and Norman Sanford
National Institute of Standards and Technology, Gaithersburg, Maryland 20899

Pavel Mogilevsky

Air Force Research Laboratory, Materials and Manufacturing Directorate, Wright-Patterson AFB,
Ohio 45433-7817

(Received 28 February 2005; accepted 18 July 2005; published online 31 August 2005)

Growth habits and defects in epitaxial ZnO nanowires grown from Au catalyst on (00.1) GaN/sapphire substrate using the vapor-liquid-solid (VLS) technique were studied using electron microscopy and x-ray diffraction. The results revealed presence of both horizontal (crawling-like) and vertical nanowires having similar orientation relationship to the substrate $(00.1)_{\text{ZnO}} \parallel (00.1)_{\text{GaN}}$, $[11.0]_{\text{ZnO}} \parallel [11.0]_{\text{GaN}}$. The crawling-like growth precedes the vertical growth, and the coalescence and overgrowth of the crawling nanowires produce a highly defective layer which separates the substrate and vertical nanorods. Transmission electron microscopy revealed a high density of planar defects in this interfacial layer. A significant density of stacking faults residing on the (0001) planes was also observed in the shorter vertical nanorods. The crawling nanowires are under residual compressive strain, whereas the vertical nanorods grow strain-free. © 2005 American Institute of Physics. [DOI: 10.1063/1.2041832]

One-dimensional semiconductor nanostructures (nanowires and nanorods), exhibiting photonic and electronic confinement in two dimensions have attracted considerable interest as potential candidates for a variety of nanoscale electronic and optoelectronic devices. Nanowires/nanorods of ZnO are particularly promising candidates for the optoelectronic devices since ZnO features a wide band gap (3.37 eV), combined with the largest excitonic binding energy (60 meV) of all semiconductors, and high optical gain (300 cm^{-1}) which facilitates the low-threshold stimulated emission required in lasers.^{1,2}

Recently, ZnO nanowires have been grown on sapphire using the vapor-liquid-solid (VLS) method,³ metalorganic vapor-phase epitaxy (MOVPE),⁴ and pulsed laser deposition (PLD),⁵ on fused silica using chemical vapor deposition (CVD),⁶ and on GaN substrates using MOVPE.⁷ Growth of ordered ZnO nanowire arrays using porous anodic alumina templates has also been achieved.⁸ In all cases, the crystallographic *c*-axis of ZnO was parallel to the nanowire/nanorod axis and perpendicular to the substrate surface. However, most recently, a horizontal VLS growth for the ZnO nanowires on the *a*-plane sapphire has also been reported⁹ with the nanowire growth direction being parallel to the $[11.0]$ direction of the substrate. Most studies of ZnO nanowires focused on the demonstration of the growth techniques and initial characterization of the nanowire electrical and optoelectronic properties, whereas little structural characterization of ZnO nanowires and their interfaces with a substrate have been reported. The present contribution describes structural characterization of ZnO nanorods grown on the (00.1) GaN/sapphire substrate from Au catalyst using the VLS approach. The major findings of this study include (i) hitherto unreported coexistence of both horizontal (crawling-like) and vertical growth modes for the nanowires/nanorods and (ii) highly defective nature of the layer of crawling nanowires, which develops on the GaN surface and separates the substrate and vertical ZnO nanorods.

ZnO nanorods for this study were grown on a commercial GaN layer (5 μm thick) on the *c*-plane sapphire; prior to the growth, a 7 nm layer of Au was deposited using an e-beam evaporation on the GaN surface. ZnO was grown in a quartz tube furnace using a mixture of ZnO and graphite powders. Similar amounts of zinc oxide (99.999% purity) and graphite (99.99%) were ground together (total mixture weight of 0.1 g) and placed in a Si boat in the center of the tube furnace. The Au-coated GaN/sapphire substrate was placed 6 cm downstream from the boat containing the ZnO-graphite mixture. The furnace was purged with Ar (0.50 l/min) for 15 min before ramping the temperature to 900 °C (heating rate 109 °C/min) followed by a 20 min dwell under Ar flow (0.5 l/min).

The cross-sectional samples for transmission electron microscopy were prepared using both (i) focused ion beam (FIB) FEI (Ref. 10) Dual Beam 235 system and (ii) conventional sectioning and grinding, followed by ion-thinning in a Gatan Precision Polishing System (PIPS). The samples were examined in a JEOL 3010-UHR transmission electron microscope operated at 300 kV and in Hitachi-4700 FESEM.

SEM (Fig. 1) and XRD (Fig. 2) confirmed presence of ZnO nanorods having their $[00.1]$ growth axis perpendicular to the substrate surface. The nanorods, 200 nm to 500 nm long, featured Au caps as expected for the VLS growth with the ZnO growing from the ZnO-saturated Au-melt.^{11,12} In addition to vertical nanorods, the SEM images (Fig. 1) revealed the nanowires crawling over the substrate surface. The SEM images suggest that these crawling nanowires also emerged from the ZnO-saturated Au melt and continued to grow by pushing the Au-droplet along the GaN surface. In the absence of Au-particles, no deposition of ZnO on the GaN surface was detected. The crawling nanowires developed a rough discontinuous layer on the substrate surface (Fig. 1). At certain points [e.g., indicated by the white arrows in Fig. 1(a)], the crawling growth mode changed to the vertical growth with the separation of the Au-droplet from the

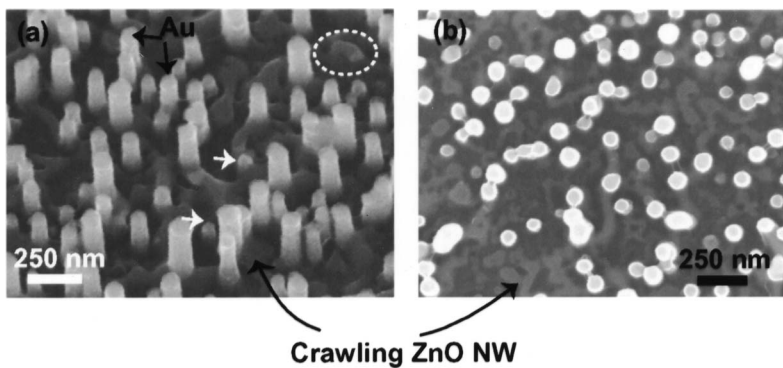


FIG. 1. SEM images of the ZnO nanorods grown on the (0001) GaN surface. (a) The sample was tilted by 25° with respect to the incident electron beam and the detector. (b) Zero sample tilt. The layer of crawling ZnO nanowires is visible in both images. An example of the crawling nanowire having Au-droplet at one end is encircled with a dashed line. Examples of vertical ZnO nanorods at the initial stages of their growth are indicated using white arrows.

substrate surface. Formation of similar crawling nanowires can also be seen in the SEM images reported previously for the ZnO nanowires VLS-grown on *a*-plane sapphire,³ which indicates that the crawling growth mode of ZnO nanowires is not specific to the GaN substrate. Our preliminary results on separate samples indicate that the crawling nanowires grow along the $\langle 1\bar{1}.0 \rangle$ directions of GaN.¹³

XRD scans across the 00.2, 00.4, 00.6, and 10.5 reflections of GaN and ZnO yielded sharp diffraction peaks corresponding to the weakly compressed GaN ($a=3.180 \text{ \AA}$, $c=5.186 \text{ \AA}$) and strain-free ZnO ($a=3.246 \text{ \AA}$, $c=5.207 \text{ \AA}$). The sharp ZnO peaks were attributed to the vertical ZnO nanorods. Rocking curve measurements utilizing the 00.2 reflections of ZnO and GaN yielded a full-width-at-half-maximum (FWHM) of 0.314° and 0.149° , respectively. Additional broad XRD peak, observed on the low-angle side of the relaxed ZnO 00.6 and 10.5 reflections, was attributed to the layer of ZnO crawling nanowires. This layer appears to be under *in-plane* compressive strain, as expected from both a thermoelastic mismatch between the ZnO and GaN/sapphire and a lattice mismatch between the ZnO and GaN.

The structural quality of the ZnO nanorods and their interfaces with the substrate were analyzed using TEM. Electron diffraction patterns confirmed that the nanorods grow on GaN epitaxially. Most vertical nanorods exhibited a flat top capped with Au [Fig. 3(a)]. Occasional nanorods having a triangular-shaped (in projection) top without Au-droplet were also observed and attributed to the fractured remains of ini-

tially longer nanorods; however, growth of such Au-free nanorods from vapor¹⁴ cannot be ruled out. Many of the nanorods exhibit a hexagonlike cross section with facets predominantly residing on the $\{11.0\}$ planes, as inferred from the TEM images of plane view cut-through-nanorods samples; these facet planes are consistent with the previous reports.¹⁵ Bright-field images of ZnO nanorods [Fig. 3(b)] recorded on the FIB-thinned cross-sectional samples reveal significant density of planar defects that extend across individual nanorods and can be attributed to the stacking faults residing on (00.1) planes. Similar densities of stacking faults have been reported recently for the MBE-grown GaN nanorods.¹⁴ The TEM images of much longer ZnO nanorods (typically found near the edges of the sample), which were separated from the substrate and dispersed on lacey carbon-coated grids, are shown in Fig. 4. In contrast to the shorter nanorods, the longer nanorods appear to be defect-free.

Cross-sectional TEM images also show a nearly continuous layer of ZnO on the GaN surface [Figs. 3(a) and 5(a)]. The layer is about 5–20 nm thick and connects individual ZnO nanorods. The layer exhibits a rough surface and the ridges connecting the nanorods are readily visible in the TEM images. This interfacial layer corresponds to the layer of crawling nanowires observed in the SEM. Diffraction contrast [Figs. 3(a) and 5(a)] and high-resolution [Figs. 5(b)–5(d)] TEM imaging indicated that this interfacial layer contains a high density of stacking faults on the (00.1) planes described by the displacement vector $R=1/2[20.3]$ in the $[11.0]$ projection [Figs. 5(b) and 5(c)]. Such high densities of defects on the basal planes are consistent with the broad 00.6 diffraction peak from the layer of crawling ZnO nanowires observed by the XRD (Fig. 2). Additionally, the ZnO layer features a high incidence of vertical (normal to the substrate)

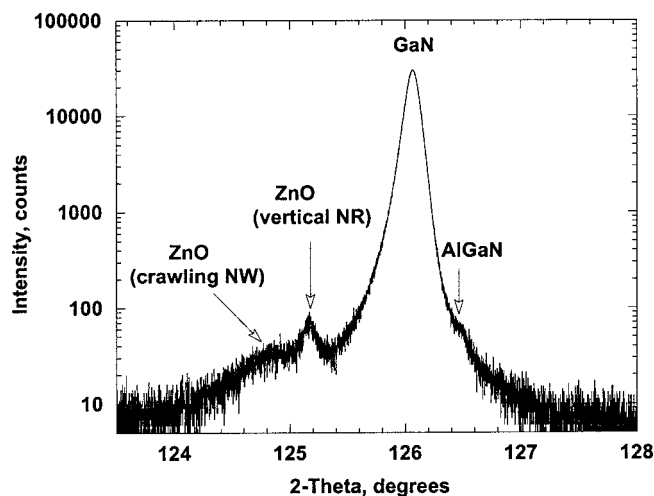


FIG. 2. XRD scan across the 0006 reflections of the ZnO and GaN. The sharp ZnO peak corresponds to the strain-free vertical nanorods. The broad ZnO peak was attributed to a layer of crawling nanowires. This layer is under residual compressive strain.

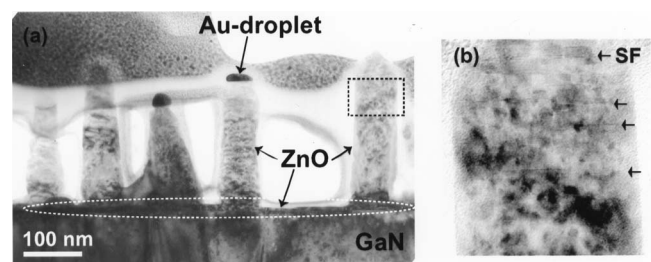


FIG. 3. (a) TEM cross-sectional image of the ZnO nanowires/nanorods on the GaN substrate. A nearly continuous interfacial layer of ZnO separating vertical ZnO nanorods and GaN substrate is indicated using white dashed line. (b) Magnified view of the rectangular area in (a). This image of a single nanorod reveals significant density of stacking-fault (SF) like defects which reside on the (0001) planes.

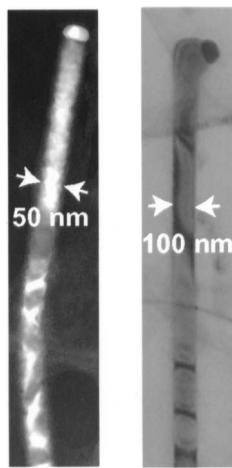


FIG. 4. TEM images of top portions of the longer ZnO nanorods separated from the substrate.

interfaces separating regions which differ by the translation $R=1/2c$ [Fig. 5(c)]. These interfaces appeared strongly inclined to the image plane, which is consistent with them being parallel to the $\{11.0\}$ planes oriented at 60° with respect to the image. Similar types of translational interfaces on both (00.1) and $\{11.0\}$ planes have been reported previously for the GaN.^{16,17} High densities of these defects, often observed in GaN films in the vicinity of GaN/substrate interface, have been attributed to the coalescence and overgrowth of three-dimensional islands, which differ by a translation with respect to the reference (e.g., substrate) lattice.¹⁷ Our observations suggest similar effects for the ZnO nanowires crawling on the GaN surface. We conclude that the crawling growth precedes the vertical growth and creates a highly defective interfacial layer separating the vertical nanorods from the substrate.

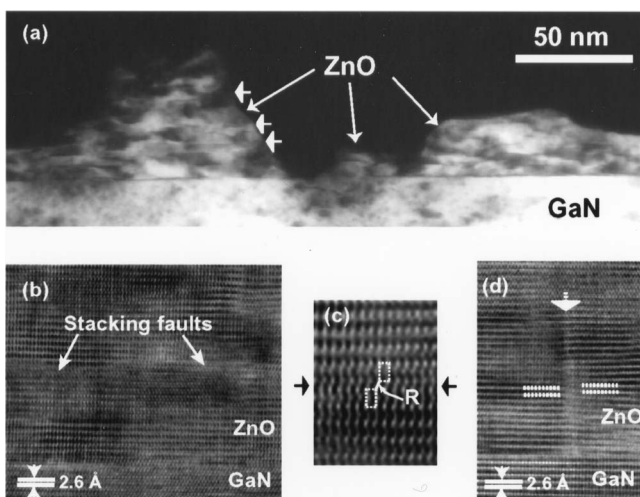


FIG. 5. (a) TEM cross-sectional dark-field image of the interfacial ZnO layer. The image reveals a high density of planar defects. (b)–(d) HRTEM images of planar defects in the interfacial layer. (b), (c) Stacking-faults residing on the (00.1) planes. The displacement vector R is indicated in (c). (d) Planar translational interface (indicated by arrows) residing on the $\{11.0\}$ planes inclined at 60° to the image plane.

HRTEM images of the ZnO/GaN interfaces analyzed by fast Fourier transform filtering revealed the presence of misfit dislocations. The spacing between dislocations corresponding to a completely relaxed layer was estimated¹⁶ as $L=(d_1+d_2)^2/4(d_1-d_2) \approx 14.4$ nm, where $d_1=d_{(1\bar{1}.0)\text{GaN}}=0.277$ nm, and $d_2=d_{(1\bar{1}.0)\text{ZnO}}=0.281$ nm. The spacing between the misfit dislocations observed experimentally varied among different regions but typically was close to 14 nm indicating that the epitaxial strain in ZnO is largely relaxed. Therefore, the compressive strain in the crawling nanorods inferred from XRD must be dominated by the thermoelastic mismatch between the ZnO and GaN/sapphire substrate.

A recent report on the VLS growth of aligned horizontal ZnO nanowires⁹ on the a -plane of sapphire indicated that the horizontal growth mode was very sensitive to both the size of metal catalyst particles and the interparticle spacing. In particular, smaller particle sizes were observed to promote horizontal growth of ZnO nanowires preferentially along the $[1\bar{1}.0]$ direction of sapphire, whereas larger particle sizes yielded random growth directions. The exact fundamental reasons which define the balance between the crawling and vertical VLS growth modes of nanowires/nanorods have yet to be established.

In summary, our results demonstrate that the unintentional crawling-like VLS growth of nanowires which occurs prior to vertical growth generates a highly defective strained interfacial layer between the vertical nanorods and the substrate. The high density of defects in this interfacial layer is likely to affect electrical properties of the nanorods/substrate heterostructure. Crawling-like growth appears to interfere with the initial stages of vertical growth causing relatively high densities of planar defects in the bottom of the vertical nanorods.

P.M. acknowledges support from UES, Inc. under AF Contract No. F33615-01-C-5214.

¹Y. Chen, D. M. Baghall, H. Koh, K. Park, K. Hiraga, Z. Zhu, and T. Yao, *J. Appl. Phys.* **84**, 3912 (1998).

²A. Ohtomo, M. Kawasaki, Y. Sakurai, I. Ohkubo, R. Shiroki, Y. Yoshida, T. Yasuda, Y. Segawa, and H. Koinuma, *Mater. Sci. Eng., B* **56**, 263 (1998).

³M. H. Huang, S. Mao, H. Feick, H. Yan, Y. Wu, H. Kind, E. Weber, R. Russo, and P. Yang, *Science* **292**, 1897 (2001).

⁴W. I. Park, D. H. Kim, S. W. Jung, and Gyu-Chul Yi, *Appl. Phys. Lett.* **80**, 4232 (2002).

⁵M. Kawakami, A. B. Hartanto, Y. Nakata, and T. Okada, *Jpn. J. Appl. Phys., Part 1* **42**, L33 (2003).

⁶J.-J. Wu and S.-C. Liu, *Adv. Mater. (Weinheim, Ger.)* **14**, 215 (2002).

⁷W. I. Park and Gyu-Chul Yi, *Adv. Mater. (Weinheim, Ger.)* **16**, 87 (2004).

⁸C. Liu, J. A. Zapien, Y. Yao, X. Meng, C. S. Lee, S. Fan, Y. Lifshitz, and S. T. Lee, *Adv. Mater. (Weinheim, Ger.)* **15**, 838 (2003).

⁹B. Nikoobakht, C. A. Michaels, S. J. Stranick, and M. D. Vaudin, *Appl. Phys. Lett.* **85**, 3244 (2004).

¹⁰The use of brand or trade name does not imply endorsement of the product by NIST.

¹¹M. H. Huang, Y. Wu, H. Feick, N. Tran, E. Weber, and P. Yang, *Adv. Mater. (Weinheim, Ger.)* **13**, 113 (2001).

¹²S. Y. Li, P. Lin, C. Ying, and T. Y. Tseng, *J. Appl. Phys.* **95**, 3711 (2004).

¹³A. Davydov, B. Nikoobakht, I. Levin, and N. Sanford (to be published).

¹⁴T. Araki, Y. Chiba, and Y. Nahishi, *J. Cryst. Growth* **210**, 162 (2000).

¹⁵Y. Ding, P. X. Gao, and Z. L. Wang, *J. Am. Chem. Soc.* **126**, 2066 (2004).

¹⁶P. Ruterano and G. Nouet, *Phys. Status Solidi A* **227**, 177 (2001).

¹⁷L. A. Bendersky, D. V. Tsvetkov, and Y. V. Melnik, *J. Appl. Phys.* **94**, 1676 (2003).